

MODELING THE THERMAL PERFORMANCE OF FALLING PARTICLE RECEIVERS SUBJECT TO EXTERNAL WIND

Brantley Mills, Reid Shaeffer, Clifford K. Ho, and Lindsey Yue
Sandia National Laboratories
Albuquerque, New Mexico, 87185-1127, USA
bramill@sandia.gov

ABSTRACT

Falling particle receivers (FPRs) are an important component of future falling particle concentrating solar power plants to enable next-generation energy generation. High thermal efficiencies in a FPR are required to high thermodynamic efficiencies of the system. External winds can significantly impact the thermal performance of cavity-type FPRs primarily through changing the air flow in and out of the aperture. A numerical parametric study is performed in this paper to quantify the effect of wind on the thermal performance of a FPR. Wind direction was found to be a significant parameter that can affect the receiver thermal efficiency. The particle mass flow rate did not significantly change the overall effect of wind on the receiver. The receiver efficiency was strong function of the particle diameter, but this was primarily a result of varying curtain opacity with different diameters and not from varying effects with wind. Finally, the model was used to demonstrate that receiver efficiencies of 90% were achievable under the assumption that the effect of wind/advective losses were mitigated.

Keywords: concentrating solar power, falling particle, receiver, thermal efficiency, wind, simulation.

1. INTRODUCTION

Among the candidates for next generation concentrating solar power (CSP), falling particle technology is a promising contender to deliver sustainable baseload energy generation [1,2]. Falling particles offer numerous advantages over more traditional CSP designs including: the ability to directly irradiate the heat transfer medium over a larger temperature range, the use of a low-cost, commercially available medium, and the enabling of long-term energy storage of the particles during off-peak hours. In particular, the ability to directly irradiate falling particles facilitates higher temperatures and higher overall thermal efficiencies without the need to consider structural

temperature limits that are normally required to safely confine the heat transfer medium.

The falling particle receiver (FPR) is a critical component to consider in a CSP falling particle system in order to achieve high thermal efficiencies. Receiver efficiencies of ~90% have been targeted with particle outlet temperatures >700°C for existing falling particle receiver designs, and many of these designs have focused on cavity receivers that limit losses both radiatively and convectively. Cavity type receivers also have the advantage of providing more obstructions to external winds on the falling particle curtain.

At the National Solar Thermal Test Facility (NSTTF) at Sandia National Laboratories (SNL), a north-facing cavity FPR has been tested and shown to achieve particle outlet temperatures >700°C [3]. However, despite more precise control of the particle mass flow rate [4], a recent series of tests and subsequent analysis [5] has suggested that external winds and advective losses out of the cavity aperture must be mitigated to achieve the target thermal efficiencies. Several strategies have been identified to mitigate these effects and are the subject of present research, but a study of the effects of wind on this present receiver design is necessary to evaluate the effectiveness of these strategies.

Previous studies have been performed on FPRs of different sizes to identify the relevant effects from wind speed and direction [6,7,8]. Tan et al. [7] found that, for some wind directions, efficiency can be improved by inhibiting hot air from escaping the receiver. However, these results are often very dependent on the shape of the cavity and a hopper might be excluded that could otherwise affect the flow in and out of the cavity. Flesch et al. [8] performed an experimental analysis of a cavity receiver oriented in different directions under the influence of wind. By matching relevant dimensionless numbers with a scaled cavity model in a wind tunnel, it is suggested that horizontal receivers are less sensitive to wind, however suffer

from increased advective losses. Conversely receivers with apertures biased downward exhibited lower advective losses overall at the expense of increased wind sensitivity.

A complementary analysis of these works is performed in this paper using an existing computational fluid dynamics (CFD) model developed in ANSYS Fluent® to evaluate the effect of wind on the thermal performance of an existing, well-defined FPR design with dimensions similar to those at the NSTTF. This study helps to inform future design efforts of the most critical wind conditions that affect the receiver performance.

To reduce computational resource requirements, the effect of the supporting structures external to the receiver on wind and receiver performance is neglected. Despite this assumption, several important conclusions are still gleaned about the effect of wind on FPRs. Future modeling efforts are underway to complement this study. These efforts will enable the use of higher fidelity models of the receiver by taking advantage of Sandia's High-Performance Computing (HPC) platforms. This future modeling strategy is also more suitable for large scale parametric studies that can guide future solar receiver design and wind mitigation strategies.

The remainder of this paper is organized as follows. First, the physics implemented in the CFD model are described. Next, the model's spatial discretization and domain size are varied to support the number of elements used and extent of the boundaries, respectively. Then, the effect of wind on the receiver efficiency is computed at various wind speeds and directions. The analysis is repeated for different particle mass flow rates and for different particle sizes. Then, the model is used to evaluate the efficiency of the receiver if wind and advective losses were mitigated. Finally, the results and future work are summarized.

2. COMPUTATIONAL MODEL

The follow section describes the computational model that was utilized to investigate the effect of external wind on a FPR. Solution verification tests were also performed to confirm sufficient spatial discretization and mesh domain size.

2.1 Model Description

A CFD model of a previously tested FPR design at the NSTTF was utilized to study the effect of wind. This model, developed in ANSYS Fluent®, has been discussed thoroughly in the literature [5,9,10], but a brief summary of the modeling strategy is provided here for reference. A solid model of the receiver itself is depicted in Figure 1.

The air volume inside and outside the receiver were modeled with a nominal domain size of 14x14x10 m. Conduction through the mostly Duraboard® receiver walls (as shown in Figure 1) was modeled, and the receiver walls were convectively and radiatively coupled with the surrounding environment. Lagrangian particles were released in a curtain with the same dimensions and at the same location as the particle curtain used at the NSTTF FPR. The particles fell through the domain under the force of gravity and were coupled with the surrounding air through drag and heat transfer. The realizable k-ε turbulence model [11] was applied using Fluent's 'scalable' wall functions to be more robust at the wall with regards to varying mesh size.

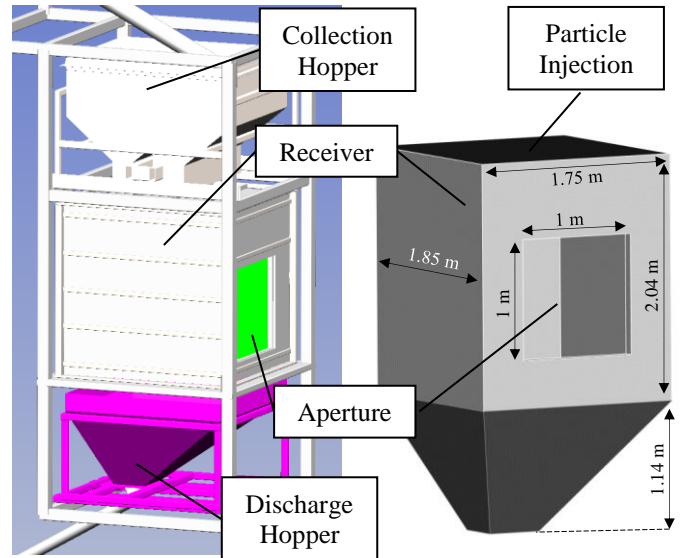


Figure 1. Solid model of the NSTTF receiver (left) and the solid geometry used in the parametric study (right)

The particles exited the domain when they came into contact with the hopper walls at the bottom of the receiver. Note that particle bouncing was not included in the model to limit computational expense. The particles used in the model, CARBO HSP (82% Al₂O₃, 5% SiO₂, 3.5% TiO₂) with ~7% iron oxide and particle diameters of 350 μm, were those that were used at the NSTTF, and their material properties were taken from Reference [12]. Particle to particle interaction was not included under the assumption that the particle volume fraction is less than 10% which has been established for other FPRs [13].

A non-grey discrete ordinates (DO) radiation model was coupled with the CFD model to include the effects of the incident solar radiation from the heliostat field and thermal emissions. The radiation was divided into three bands: 0.1 – 2.5 μm, 2.5 – 4.5 μm, and 4.5 – 100 μm. The incident radiation enters entirely in the smallest wavelength band; the two larger bands are indicative of thermal emissions. The distinction in the thermal wavelengths is used to account for differences in the emissive properties of Duraboard®. Note the radiative losses from the smallest wavelength band is more representative of reflected solar radiation out of the domain.

Incident solar radiation to the domain was defined using the NSTTF heliostat field as the nominal case providing approximately 1 MW/m² of radiative power to the receiver. The entire aperture is defined to emit concentrated solar radiation with a flux profile determined from measurements taken during a representative NSTTF experiment. The incident beam direction emitted from a cell face on the aperture was determined using the method described by Khalsa and Ho [14].

2.2 Solution Verification

To provide more confidence in the results of the parametric study, two verification tests were performed on the model. First, the model was confirmed to have adequate spatial resolution using a series of meshes with an increasing number of elements.

Next, the model was confirmed to have an adequate domain size such that the boundary conditions don't adversely affect the solution. For this study, a series of meshes were generated using a comparable element size from the discretization study for various domain sizes.

For the spatial discretization study, cell size varied considerably throughout the mesh depending on the proximity to walls. Therefore, as a surrogate for cell size, the total number of cells was evaluated for a nominal domain size of 14x14x10 m (where the smaller dimension is the top/bottom dimension). Six hexahedral meshes were then generated with total number of cells ranging from 1.673×10^5 cells to 2.364×10^6 . The thermal efficiency of the receiver is then plotted against the number of cells in Figure 2, where the vertical dashed line indicates the number of elements chosen nominally.

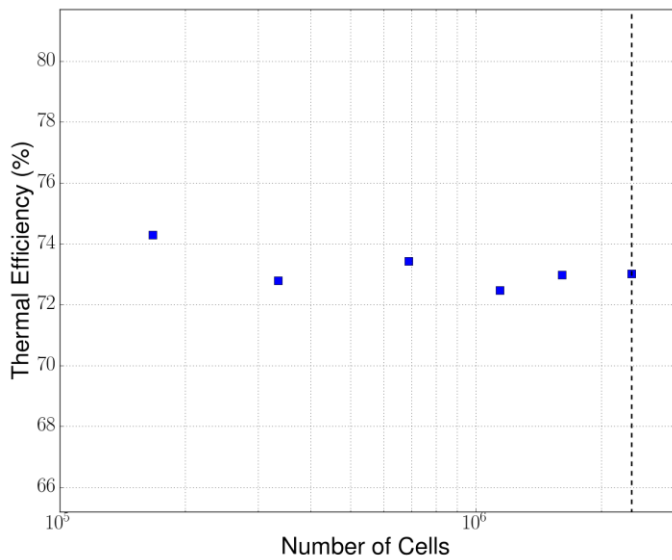


Figure 2. Receiver efficiency versus the number of cells in the mesh

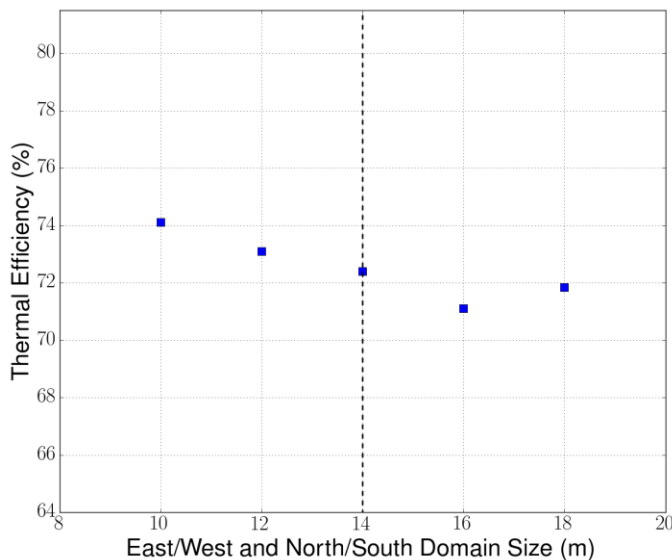


Figure 3. Receiver efficiency versus the domain size of the model

As shown in Figure 2, the spatial discretization of the geometry is more than sufficient to adequately resolve the physics. Likewise, the thermal efficiency is plotted for a series of meshes of various domain sizes ranging from the smallest size of 10x10x6 m to the largest size 18x18x14 m. For each successive mesh, the domain size is increased by 2 m for each coordinate direction. The results are plotted in Figure 3, where the vertical dashed line again indicates the nominal domain size. As before, the plot indicates the nominal domain size is sufficient (likely within other unquantified numerical uncertainties) to not adversely affect the solution from the boundaries.

3. PARAMETRIC WIND STUDY

To ascertain the effects of wind on the thermal performance of this FPR, a parametric study is pursued investigating a range of wind speeds and directions. This being a north-facing receiver, requires that directions from North to South are considered. Receiver operating conditions are evaluated from the set of NSTTF experiments, resulting in the following nominal conditions used in this analysis: an average, incident radiative flux of 1.04 MW/m^2 , inlet particle temperatures of 600°C , and particle mass flow rates of 10 kg/s . This study is repeated later for a lower particle mass flow rate. Next, the effect of varying particle diameter in the curtain is also evaluated. Finally, the receiver is evaluated for conditions where the effects of external winds and advective losses are mitigated.

The thermal efficiency of the receiver is used as the primary metric to evaluate the effect of the wind. The thermal efficiency is defined as:

$$\eta_{th} = \frac{Q_a}{Q_i} = \frac{\dot{m}_p (h_{o,p} - h_{i,p})}{Q_i} = \frac{\dot{m}_p \int_{T_{i,p}}^{T_{o,p}} c_p(T) dT}{Q_i} \quad (1)$$

where Q_a was the absorbed thermal power in the particles, Q_i was the incident thermal radiative power, \dot{m}_p was the total particle mass flow rate, h_p as the enthalpy of the particles, and $c_p(T)$ was the specific heat of the particles (J/kg·K) as a function of temperature T defined as:

$$c_p(T) = 365 \cdot T^{0.18} \quad (2)$$

where T was the mean particle temperature ($^\circ\text{C}$) for $50^\circ\text{C} \leq T \leq 1100^\circ\text{C}$. Essentially, the thermal efficiency is the fraction of incident radiative power that is transferred to the particles.

The particle outlet temperature used for evaluating thermal efficiency was computed using an average of particle temperatures passing through a plane just below the aperture. Particles pass through this evaluation plane before the particles actually exit the domain at contact with the receiver wall. This location corresponds to where particle temperatures are measured in the NSTTF experiment and this keeps the reported efficiency consistent with values calculated experimentally. However, heat transfer will continue to occur as the particles continue to fall after crossing through the evaluation plane and before they exit the receiver. Therefore, the sum of the reported losses from each loss mechanism plus the efficiency may not add up to one exactly.

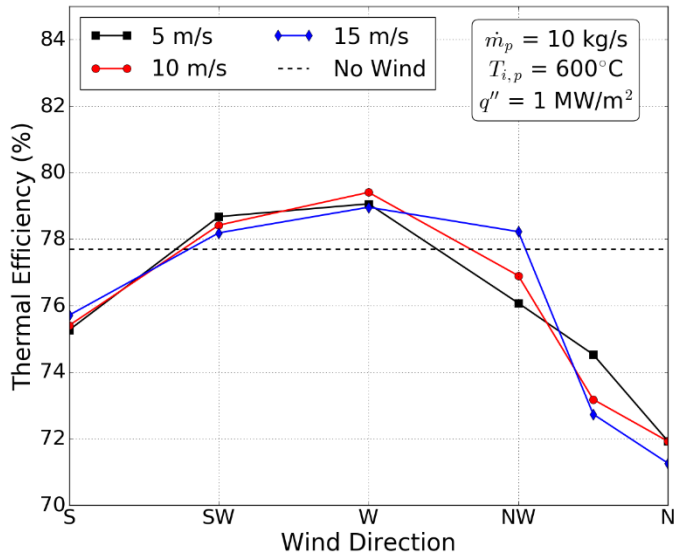


Figure 4. Receiver efficiency at various wind speeds and directions

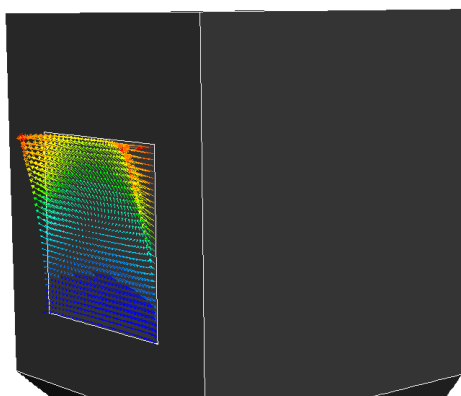
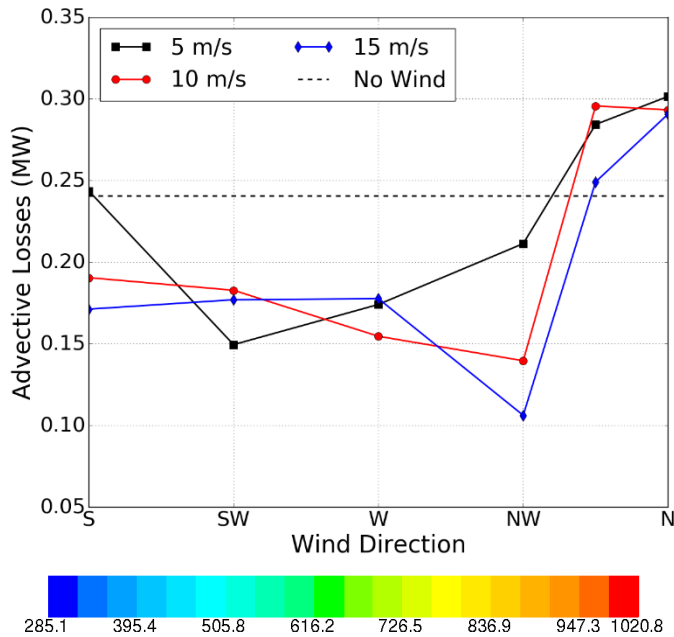


Figure 5. Advective losses at different wind speeds and directions (top) and a vector plot of air colored by temperature in K (bottom)

3.1 Effect of Wind Speed/Direction

Three separate wind speeds, 5, 10, and 15 m/s, are evaluated at six different wind directions, N, NNW, NW, W, SW, and S. This leads to a total of 18 cases and one additional case without wind to evaluate a baseline thermal efficiency of the receiver. The thermal efficiency of the receiver for each scenario is plotted against the wind direction for all explored speeds in Figure 4.

As shown in the figure, the receiver thermal efficiency is marginally affected by the wind speed for a given direction. However, the wind direction has the most significant impact on the efficiency with the most northern winds having the largest impact. To understand how wind is affecting the thermal efficiency of the receiver, the total advective losses from the receiver are plotted in Figure 5 for all wind directions and speeds. For clarity, advective losses here refer to the fraction of incident thermal power that is lost from hot air escaping the receiver aperture to be replaced by cooler ambient air. Recall that the advective losses may be larger than the losses reported by the efficiency due to how the thermal efficiency is being calculated as described above. Also shown in Figure 5 is a velocity vector plot of the air flow at the aperture colored by the air temperature for a northern wind at 10 m/s.

As shown in the Figure 5, increased advective losses for a given wind direction are inversely proportional to the thermal efficiency. This fact, coupled with the large variability in the advective losses for 1.04 MW incident power, suggests that the primary effect of wind is to change how hot air is exchanged with cooler ambient air through the aperture. However, the shape and location of the falling particle curtain is also marginally affected by the wind direction suggesting that there are secondary effects as well. The location of particle curtain as it passes through a plane just below the aperture without wind, with a N wind of 15 m/s, and with a NNW wind of 15 m/s is plotted in Figure 6. Note that this simulation does not include particle ‘fines’ which would undoubtedly be more susceptible to the effect of wind.

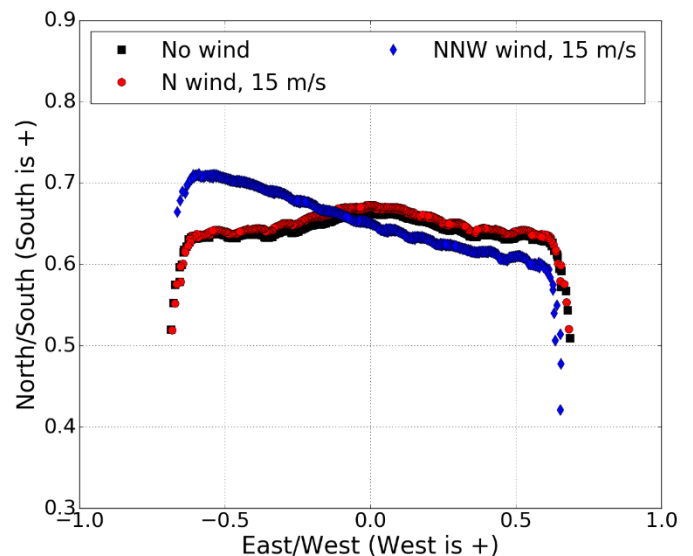


Figure 6. Particle curtain position passing through a plane below the aperture for no wind, a 15 m/s N wind, and a 15 m/s NNW wind

Implications of this finding are that (1) wind can have very complicated effects on the performance of a FPR, and (2) universal design guidance that is applicable to all receivers is difficult to find. For example, the impact of wind can be a function of structural elements around the receiver, the shape of the receiver cavity, the location of the falling particle curtain/curtains, the particle diameter, the nod angle of the aperture. As shown in other studies on the subject [7] as well as this one, external winds on a FPR can even improve the performance if the wind inhibits hot air from escaping the receiver.

3.2 Effect of Particle Mass Flow Rate and Diameter

The parametric study was repeated for the same range of wind speeds and directions using a lower mass flow rate of 5 kg/s. The results are provided in Figure 7.

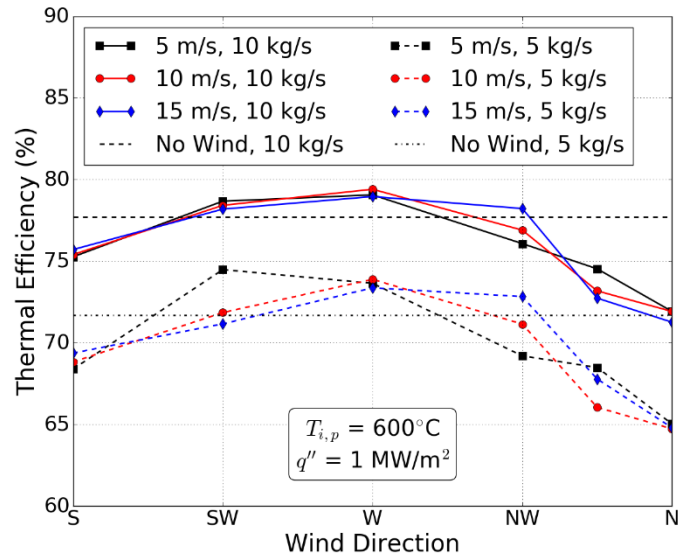


Figure 7. Effect of winds on the thermal efficiency for particle mass flow rates of 5 and 10 kg/s

Given that the falling particle curtain appeared minimally altered by the wind speed in Figure 6, it is unsurprising that the effect of wind on a 5 kg/s curtain is similar to that of a 10 kg/s curtain as shown in Figure 7. The effect of wind for all directions and speeds up to 15 m/s on the advective losses is largely the same. Ultimately, the decrease in overall performance at 5 kg/s is simply from a more transmissive falling particle curtain. This is shown in Figure 8 where the advective losses are very similar for the two particle mass flow rates.

Next, the thermal efficiency of the receiver is evaluated for four different particle diameters subject to a NNW wind of 10 m/s. The particle mass flow rate was 10 kg/s and the particle inlet temperature was 600°C. A NNW wind was chosen as it was hypothesized to have the most influence on a falling particle curtain position, but any northern wind would have been a suitable choice. Particle diameters of 200, 350, 500, and 700 μm were selected for these simulations (where the nominal values used previously were 350 μm).

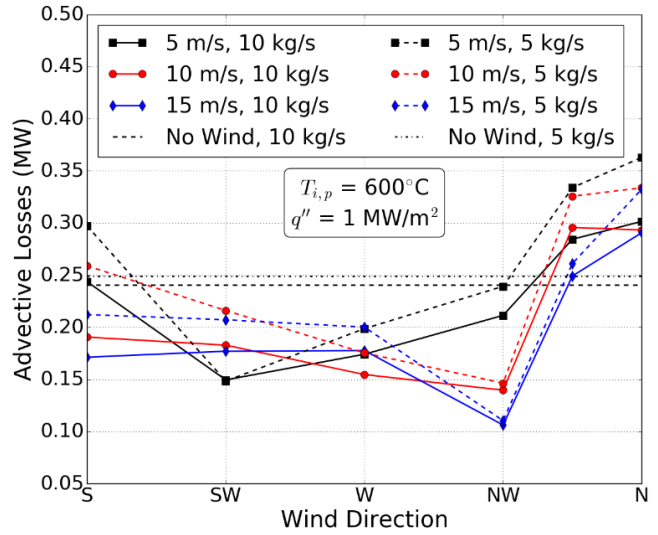


Figure 8. Advective losses at mass flow rates of 5 and 10 kg/s

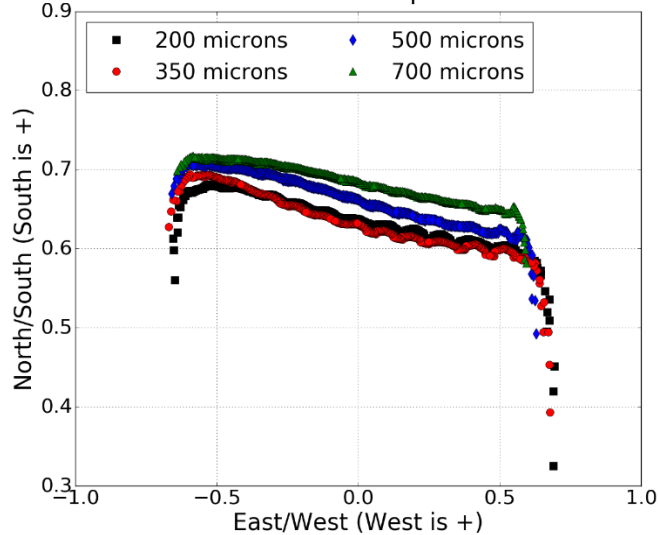
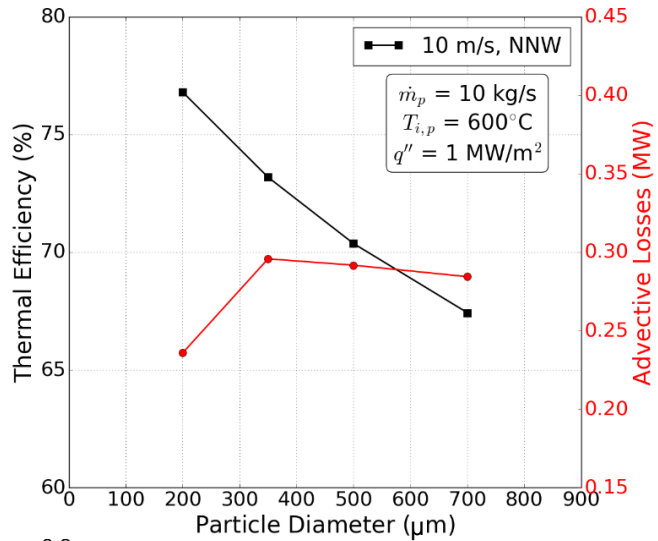


Figure 9. Effect of wind on particle diameters from 200 to 700 μm (top) and curtain position for each particle diameter (bottom)

As shown in Figure 9, the thermal efficiency of the receiver was a strong function of the particle diameters, but the gains in thermal efficiency were not a result of changes in the advective losses (except for the smallest particle diameters) or curtain position (which changed by at most 5-7 cm). Instead, the gains in efficiency were primarily a result of increased curtain opacity from smaller diameter particles for an equivalent mass flow rate which has been observed in other works in the literature [15].

3.3 Mitigating Wind/Advective Losses

Finally, additional cases are considered under the assumption that wind effects could be eliminated from the FPR design. The existing receiver model is modified such that flow in and out of the aperture is obstructed. This might be accomplished with the aid of a quartz window or forced air curtain (ignoring various effects that accompany these mechanisms), but the specific technique is not the focus of this analysis. The primary purpose is to determine the ideal receiver efficiency that might be achievable with the present design if advective losses were mitigated. Four additional simulations are performed restricting flow in and out of the aperture for particle mass flow rates of 5 and 10 kg/s and solar irradiances of 1 and 1.5 MW/m². The same receiver geometry and aperture size were used for all four simulations, and only the total power entering the aperture was increased. The thermal efficiency for each case and the thermal losses from each remaining mechanism are plotted in Figure 10.

As shown above, for nominal conditions with the effects of wind/advective losses mitigated from the receiver, the model predicts that receiver efficiencies of 90% are achievable. Several mechanisms are currently being considered to achieve these efficiencies including aperture hoods, quartz-half shells on the aperture, controlled air flow through the receiver, and recirculating air curtains over the aperture (also referred to as an aerowindow). These techniques are the focus of many present and future research efforts.

4. CONCLUSIONS

A parametric numerical study was performed using a well-developed CFD model of a north-facing FPR design previously tested at the NSTTF at Sandia National Laboratories. The purpose of this effort was to quantify the effect of wind speed and direction on the thermal efficiency of the receiver. The model was exercised for different wind speeds ranging from 5-15 m/s and all cardinal wind directions. A solution verification study was performed on the model that demonstrated sufficient spatial discretization and domain size of the model for the range of wind conditions explored.

The parametric study showed that for nominal operating conditions, the wind direction was the dominant factor affecting the thermal efficiency. The wind speed had minimal impact. The primary process through which the wind affected the thermal efficiency was through changing the advective losses though the shape of the falling particle curtain was also affected. The particle mass flow rate had a negligible impact on the effect of wind. The thermal efficiency of the receiver was a strong function of the particle diameter. However, this improvement was primarily a function of increased curtain opacity rather than

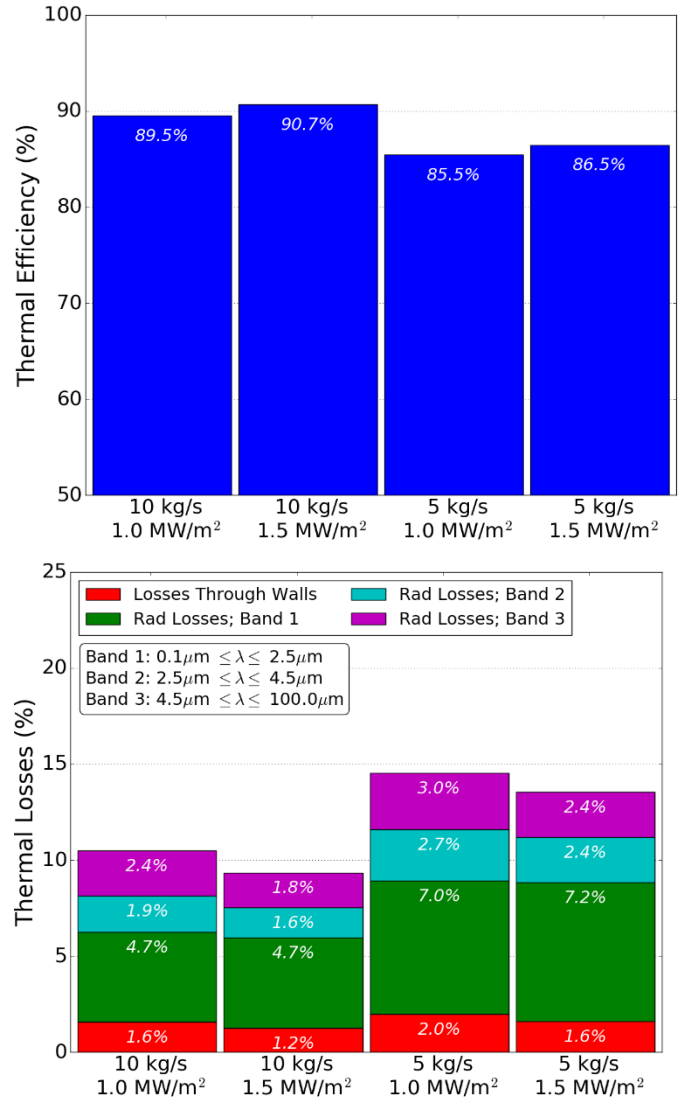


Figure 10. Receiver thermal efficiency and losses at nominal conditions mitigating the effect of wind/advective losses

from changes in the falling curtain or advective flow due to wind. Finally, the model was used to show that when wind/advective losses from the receiver are mitigated from the FPR design, receiver efficiencies of approximately 90% were achievable.

ACKNOWLEDGEMENTS

This work was funded by the DOE Solar Energy Technologies Office and Gen 3 CSP program. Sandia National Laboratories is a multi-mission laboratory managed and operated by National Technology and Engineering Solutions of Sandia, LLC., a wholly owned subsidiary of Honeywell International, Inc., for the U.S. Department of Energy's National Nuclear Security Administration under contract DE-NA0003525.

REFERENCES

[1] C. Ho, J. Christian, D. Gill, A. Moya, S. Jeter, S. Abdel-Khalik, D. Sadowski, N. Siegel, H. Al-Ansary, L. Amsbeck, B.

Gobereit and R. Buck, "Technology advancements for next generation falling particle receivers," *Proceedings of the SolarPACES 2013 International Conference*, **49** (Energy Procedia), 398 (2014).

[2] Ho, C.K., "A Review of High-Temperature Particle Receivers for Concentrating Solar Power," *Applied Thermal Engineering*, **109**, 95 (2016).

[3] Ho, C.K., J.M. Christian, J. Yellowhair, K. Armijo, and S. Jeter, "Performance Evaluation of a High-Temperature Falling Particle Receiver," in *ASME Power & Energy Conference*, Charlotte, NC, June 26-30, 2016.

[4] Ho, C. K., et al., "On-Sun Testing of a 1 MW_t Particle Receiver with Automated Particle Mass-Flow and Temperature Control," Presented at *SolarPACES 2018*, Casablanca, Morocco, October 2-5, 2018.

[5] Mills, B., Ho, C. K., "Simulation and Performance Evaluation of On-sun Particle Receiver Tests," Presented at *SolarPACES2018*, Casablanca, Morocco, October 2-5, 2018.

[6] Kim, K., Moujaes, S., Kolb, G., "Experimental and simulation study on wind affecting particle flow in a solar receiver," *Solar Energy*, **84**, 163 (2010).

[7] Tan, T., et al., "Wind effect on the performance of solid particle solar receivers with and without the protection of an aerowindow," *Solar Energy*, **83**, 1815 (2009).

[8] Flesch, R., Stadler, H., Uhlig, R., and Hoffschmidt, B., "On the influence of wind on cavity receivers for solar power towers: An experimental analysis." *Applied Thermal Engineering*, **87**, 724 (2015).

[9] Mills, B. and C.K. Ho, "Numerical Evaluation of Novel Particle Release Patterns in High-temperature Falling Particle Receivers," in *ASME Power & Energy Conference*, Charlotte, NC, June 26-30, 2017.

[10] Ho, C.K., B. Mills, and J.M. Christian, "Volumetric Particle Receivers for Increased Light Trapping and Heating", in *ASME Power & Energy Conference*, Charlotte, NC, June 26-30, 2016.

[11] T.-H. Shih, W. W. Liou, A. Shabbir, Z. Yang, and J. Zhu. "A New - Eddy-Viscosity Model for High Reynolds Number Turbulent Flows - Model Development and Validation", *Computers Fluids*, **24**(3), 227 (1995).

[12] N. P. Siegel, C. K. Ho, S. S. Khalsa and G. J. Kolb, "Development and Evaluation of a Prototype Solid Particle Receiver: On-Sun Testing and Model Validation," *Journal of Solar Energy Engineering-Trans. of the ASME*, **132**(2), (2010).

[13] Siegel, N., G. Kolb, K. Kim, V. Rangaswamy, and S. Moujaes, "Solid particle receiver flow characterization studies," *Proceedings of the Energy Sustainability Conference*, 877 (2007)

[14] Khalsa, S.S.S. and Ho, C. K., "Radiation Boundary Conditions for Computational Fluid Dynamics Models of High-Temperature Cavity Receivers," *Journal of Solar Energy Engineering-Trans. of the ASME*, **133**(3), (2011).

[15] Ho, C. K., Christian, J. M., Moya, A. C., Taylor, J., Ray, D., Kelton, J., "Experimental and Numerical Studies of Air Curtains for Falling Particle Receivers," *Proceedings of ASME 2014 8th International Conference on Energy Sustainability & 12th Fuel Cell Science*, Boston, Massachusetts, June 29-July 2, 2014.